Applied Surface Science Advances 15 (2023) 100400

Contents lists available at ScienceDirect

Applied Surface Science Advances

journal homepage: www.sciencedirect.com/journal/applied-surface-science-advances

Green synthesis of zinc oxide nanoparticles using *Pisonia Alba* leaf extract and its antibacterial activity

M. MuthuKathija [a], M. Sheik Muhideen Badhusha [a,*], V. Rama [b]

[a] Research Department of Chemistry, SadakathullahAppa College (Autonomous), Affiliated to Manonmanium Sundaranar University, Tirunelveli, Tamil Nadu, India
[b] Research Department of Chemistry, Sarah Tucker College (Autonomous), Affiliated to Manonmaniam Sundaranar University, Tirunelveli, Tamil Nadu, India

ARTICLE INFO

Keywords:
Pisonia Alba
Nanoparticles
Green synthesis
Zinc oxide
Reducing agent

ABSTRACT

The reducing and capping agent of *Pisonia Alba* leaf extract were used in a green production of zinc oxide (ZnO) nanoparticles. UV–Vis, X-ray diffraction (XRD), Fourier transform infrared spectroscopy (FTIR), and scanning electron microscopy with EDS (SEM) were all used to examine the produced ZnO nanoparticles. UV–Vis spectroscopy verified the synthesis of ZnO nanoparticles and their resulting optical characteristics. The UV–Vis spectra showed that the ZnO nanoparticles formed at an absorption peak maximum of 378 nm. Bandgap of the ZnO nanoparticles was also examining. The relevance of *Pisonia Alba* leaf extract's phenolic chemicals, alkaloids, terpenoids, and proteins in the nucleation and stability of ZnO nanoparticles was proposed by Fourier transform infrared spectroscopy (FTIR). XRD pattern compared with the standard confirmed spectrum of ZnO nanoparticles formed in the present experiments. These results provide further evidence that ZnO has a hexagonal structure (JCPDS-file: 89–1397). There appears to be no contaminants in the ZnO nanoparticles, as evidenced by the XRD pattern. Nanoparticle morphology is investigated with a SEM with EDX. Based on these morphological analyses, ZnO nanoparticles have a similar shape to aloe vera leaves. Oxidation state of the Zn was determined by XPS. The green synthesized ZnO nanopartices were used to evaluate for the antibacterial activity against gram positive and gram negative bacteria. ZnO nanoparticles have potent antimicrobial properties.

1. Introduction

Nanotechnology is a fast expanding topic of study in the today world. Due to its larger surface area than bulk materials, nanotechnology development primarily offers novel solutions in processing, including optics, electronics, food packaging etc. [1–4]. In addition, there has been a rise in interest in the development of nanotechnology to produce nanosized semiconducting materials due to their unique properties, which make them suitable materials for a wide range of applications, such as sensors, catalysts, energy storage devices, antimicrobial agents, etc. Semiconducting materials include, for example, TiO_2, CuO, SnO_2, NiO, and ZnO [5–9].

ZnO has unique semiconducting, optical, pyro, and piezo electric capabilities and is biodegradable, making it the most gifted substance known amongst these semiconducting materials. In addition, ZnO is a widely known n-type semiconducting material with a large excitonic bond and a large band gap [10–14]. Zinc oxide has a minimal toxicity and is therefore designated as "Generally Recognized as Safe" (GRAS) by the FDA [15]. Therefore, it has found applications in many different areas, including electronic transistors, catalysis, cosmetics, biosensors, food safety and packaging. ZnO potent antibacterial action has found widespread application in industry, and it also has the potential to serve as a safe and effective antibiotic substitute [16–22]. Sol-gel, infrared irradiation, pulsed laser deposition, spray pyrolysis, microwave-assisted sputtering, chemical vapour deposition and hydrothermal technique are just a few of the physical and chemical processes utilized to synthesized ZnO NPs with a variety of morphologies [23–27].

Most of these physical and chemical processes have high costs, strict pressure or temperature requirements, and use hazardous chemicals that are bad for the environment. It is essential to develop new methods of synthesis that do not negatively impact the environment or call for the usage of potentially dangerous substances. The "green synthesis," a process that is safe for the planet, has recently attracted the attention of many scientists. In contrast to previous methods, this one helps create more stable and biocompatible NPs while also being easy on the environment, cheap to implement, amenable to mass production, and devoid of unnecessary chemicals [28–33]. Synthesis of NPs is used in green methods, which involve the use of bacteria, fungi, enzymes, plants, etc.

* Corresponding author.
E-mail address: drbadhunano@gmail.com (M. Sheik Muhideen Badhusha).

https://doi.org/10.1016/j.apsadv.2023.100400
Received 9 September 2022; Received in revised form 5 March 2023; Accepted 17 March 2023
Available online 28 March 2023

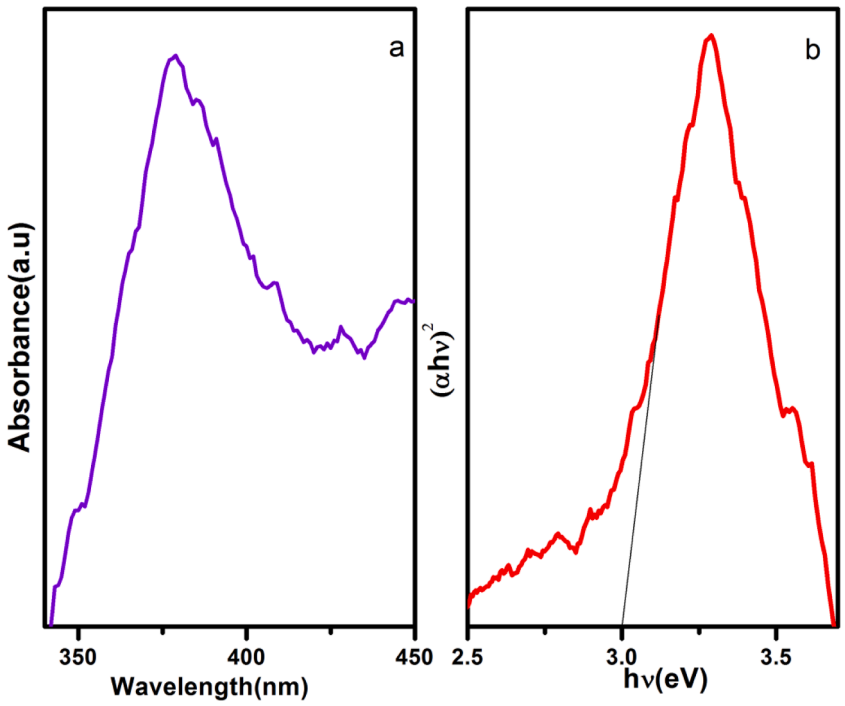

Fig. 1. UV–Vis spectra of ZnO NPs (a) absorption spectra (b) bandgap.

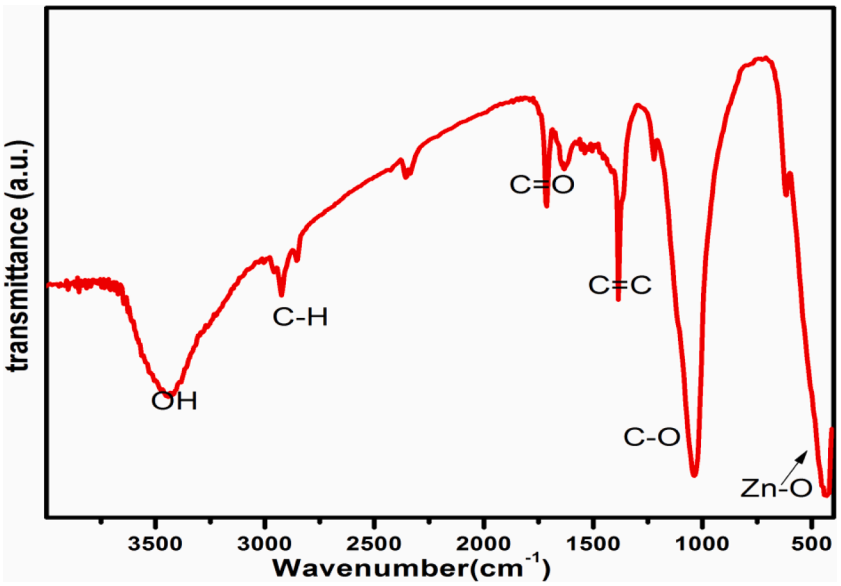

Fig. 2. FT-IR spectra of ZnONPs.

[34,35]. In addition to providing natural capping agents for the NPs, the absence of harmful compounds in these plant parts makes them an ideal platform for NPs synthesis. The method of interaction between the plant-mediated produced NPs and their environment makes them more stable and effective antibacterial agents than synthetic and natural compounds [36].

Plants like *Azadirachta indica* [37], *Hibiscus subdariffa* [38], *Syzygium cumini* [39], *Ixoracoccinea* [40], *Cassia Fistula* [41], and *Moringa oleifera* [42] have all been used to synthesis ZnO NPs as shown in the previous literatures. ZnO NPs is prepared through variety of plant materials. And first time the ZnO NPs is prepared through *P. alba* leaf extracts. *P. alba*, a member of the *Nyctaginaceae* family, is a popular crop in Southeast Asian countries like India, Sri Lanka, and the Philippines. *P. alba* leaves has been used as folk medicine It has been found to be useful in the treatment of arthritis, blood pressure, diabetes, asthma, skin thickening and anxiety. *P. alba* leaves are mostly used to treat wound healing, rheumatism, and arthritis. Phytochemicals in *P. alba* such as D. pinitol, phytol, and stigma sterol have been used for the treatment of arthritis and wound healing. These Phytochemicals have attracted us to use them as reducing and stabilizing agents for the synthesis [49]. *P. alba* has been employed for its larvicidal and ovicidal qualities, as well as its anticancer effects [43]. The purpose of this research is to create ZnO NPs using *P. alba* aqueous extract and to characterized them. Additionally, the disc diffusion method was used to test the antibacterial activity of produced ZnO NPs against a panel of harmful bacteria.

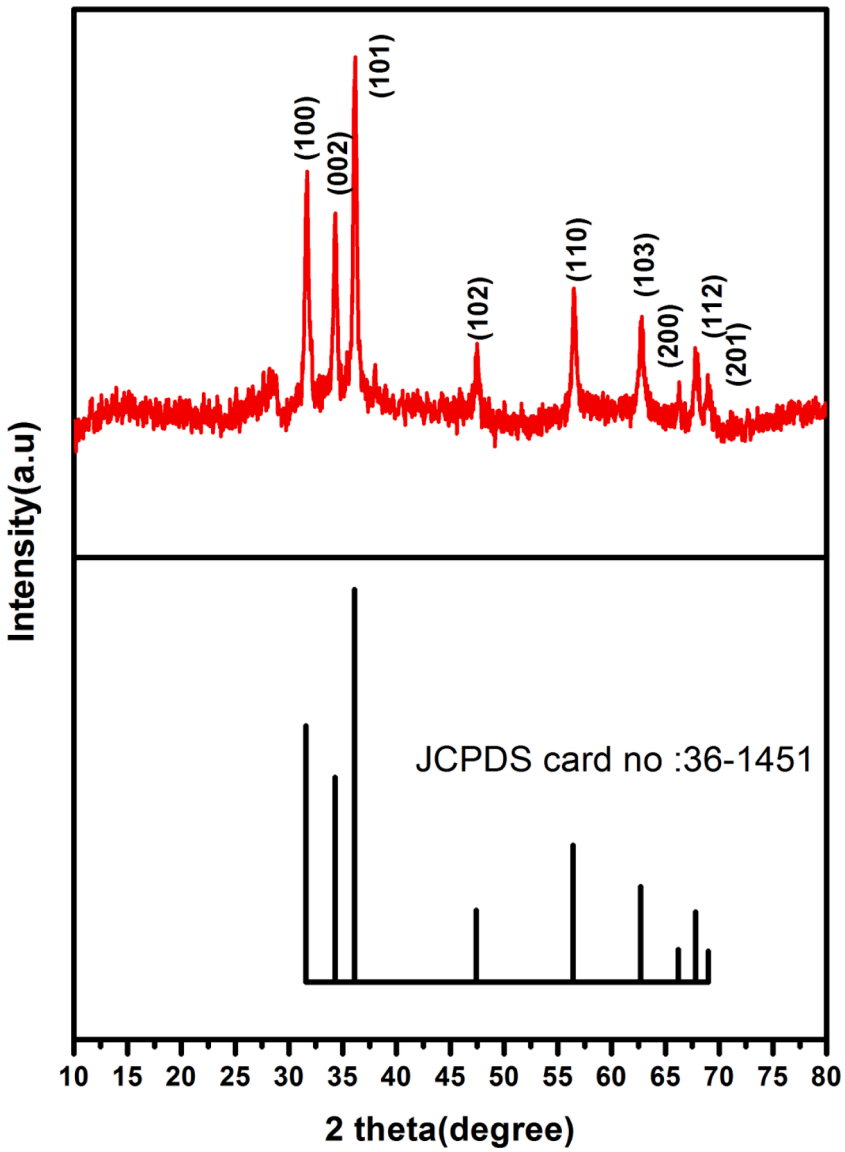

Fig. 3. XRD pattern of ZnO NPs.

2. Materials and method

2.1. Materials

Leaves of *P. Alba* were gathered in India's Tamil Nadu region, namely the Tirunelveli District. Zinc acetate dihydrate and ethanol were purchased from Merck, India Pvt. Ltd. As a solvent, deionized water was employed.

2.2. Preparation of leaf extract

All of the dust and dirt was removed from the collected *P. alba* leaves by giving them a through washing in clean water. The powdered form of dried leaves was achieved by grinding them to a fine powder. 10 g of the dried powder were boiled with 50 mL of water and extracted under reflux condition at 100 °C for 2 h. The aqueous leaves extract was made by filtering the mixture after two hours using whatmann No. 1 filter paper. Before being used in the production of ZnO NPs, the aqueous extract was chilled to 4 °C in a refrigerator.

2.3. Green synthesis of ZnO NPs

About 0.1 M zinc acetate dihydrate were dissolved in 50 mL of deionized water under constant stirring at room temperature for 15 min. After that, the zinc acetate solution was added to a 20 mL of aqueous extract of leaf solution. For two hours at 70 °C, the resultant mixture was swirled vigorously in a magnetic stirrer. When the reaction was complete, the resultant precipitate was allowed to settle, and it had taken. The precipitate was separated from the reaction solution by centrifuging at 6000 rpm for 15 min. Subsequent washings in deionized water removed any trace of impurities before drying in an air oven at 80 °C. Following synthesis, the sample was calcined for two hours at 500 °C within a muffle furnace. The ZnO NPs were powdered after drying and stored in an airtight container.

2.4. Characterization of ZnO NPs

The UV–visible absorption spectrum of ZnO NPs between 200 and 700 nm was analysed using a ELICO S1164. KBr pellets with a wavenumber range of 400 to 4000 cm^{-1} were used in the FT-IR analysis, performed on aa Thermo Nicolet 380 FTIR spectrophotometer. We determined the crystalline size and structural property of the ZnO NPs

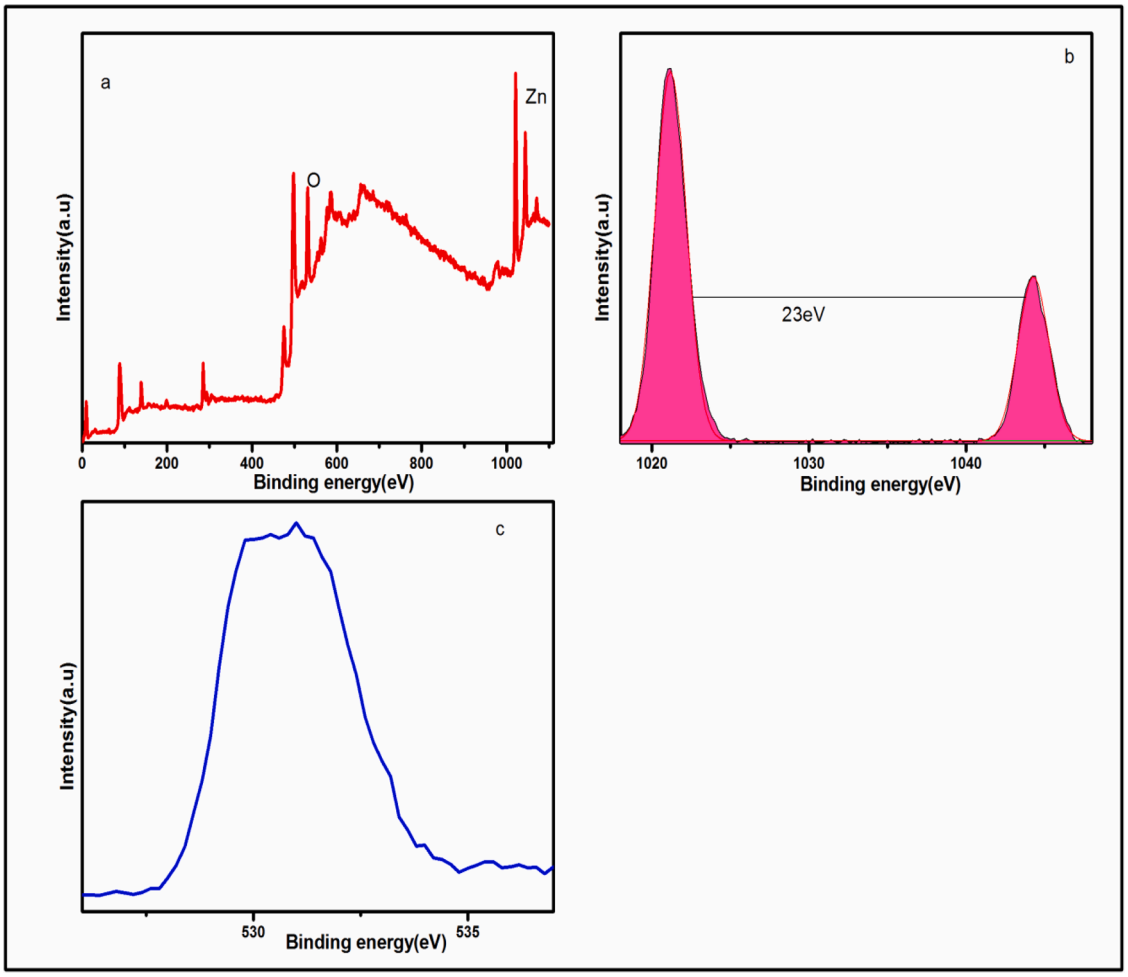

Fig. 4. XPS analysis of ZnO NPs (a) survey (b) Zn2p core level binding energy spectra (c) O1s region.

using a Pananalytical XPert PRO-powder X-ray diffractometer with Cu-K radiation(K = 1.54060 Å). The morphology of the sample was analysed using a Quanta FEG-250 SEM. We investigated the oxidation status of ZnO NPs with a PHI - VERSAPROBE II XPS spectrometer.

2.5. Antibacterial activities

Using the disc diffusion method, the bio-synthesized ZnO NPs antibacterial activity was studied against gram-positive bacteria like *Staphylococcus aureus* and gram-negative bacteria like *Klebsiella pneumoniae*. The pathogenic microorganisms were inoculated in a separate nutrient broth and incubated at 37 °C for 12 h. Test pathogenic cultures were swabbed in Muller-Hinton agar (MHA) plates after growing in a petri dish overnight. After that, 50, 75 and 100 μg/ml of ZnO NPs (all produced) were put into the disc, with water serving as a control. The plates were left in an incubator at 37 °C for a full day before the inhibition zone was measured.

3. Result and discussion

P. alba extract was used for the first time in ZnO NPs production. Polyphenols found in higher concentrations in *P. alba* lead to the production of ZnO NPs. Plant metabolites are used in a complex formation with zinc ions during this nanoparticle production. These compounds are directly decomposed into ZnO NPs at temperatures of 500 °C.

3.1. UV-Vis spectra of ZnO NPs

Characterizing the optical characteristics of synthesized NPs is a common practice, and UV–vis spectroscopy is a common method for doing so. The biosynthesized ZnO NPs UV–vis absorption spectra are displayed in Fig. 1a. Band-gap absorption of ZnO NPs due to electron transitions between the valence and conduction bands was clearly observed to have an absorption peak at 375 nm (which is very close to the bulk absorption of ZnO). These findings provided further evidence that *P. Alba* leaf extract-synthesized ZnO NPs formed (zinc acetate converted into ZnO NPs) Using Tauc's figure, one may determine the energy gap of the ZnO NPs. Extrapolating the linear portion of the of $(\alpha h\upsilon)^2 Vs\ h\upsilon$ plot, as shown in Fig. 1b, yields the optical band gap energy. The band gap energy of the ZnO NPs was found to be 2.96 eV. The reduction in the band gap value can be attributed to the effect of native defects (zinc interstitials and oxygen vacancies), which produce localized electronic states within the energy gap.

3.2. FT-IR spectra of ZnO NPs

FTIR analysis was performed to determine the functional groups present in the synthesis of ZnO NPs. In Fig. 2, the peak observed at 3444 cm^{-1} is due to the O–H stretching. An absorption peak at the region of 2929 cm^{-1} indicates the presence of the –C–H stretches of the alkyl (methyl) group. The peaks at 1717 cm^{-1} is due to the presence of stretching vibrations of C=O bond due to non-ionic carboxylic groups and may be assigned to carboxylic acids or their esters [16]. The peaks of observed at 1640 cm^{-1}due to, are assigned to the N–H bending vibration

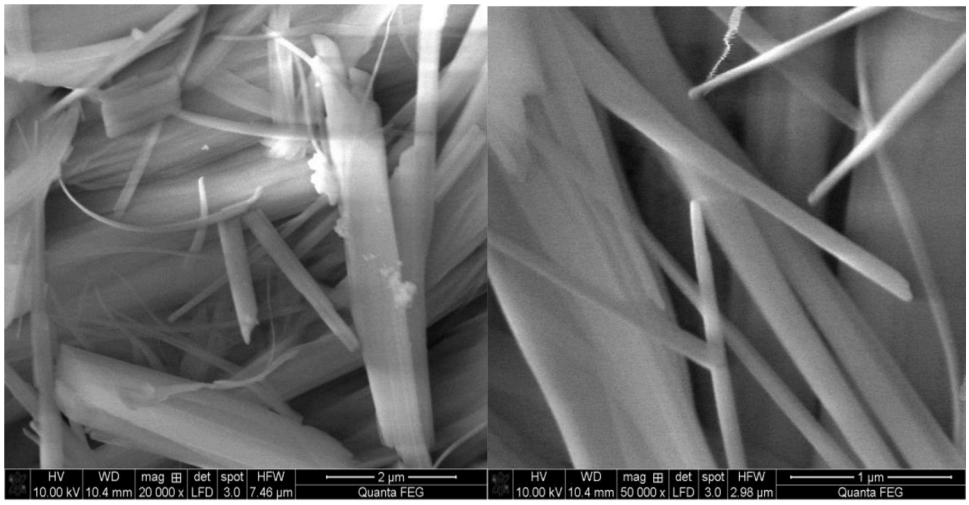

a.SEM images of ZnONPs

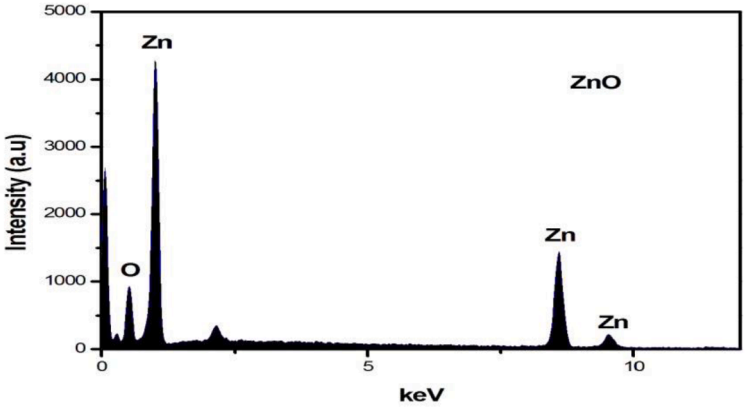

b.EDS images of ZnONPs

Fig. 5. a.SEM images of ZnONPs b.EDS images of ZnONPs.

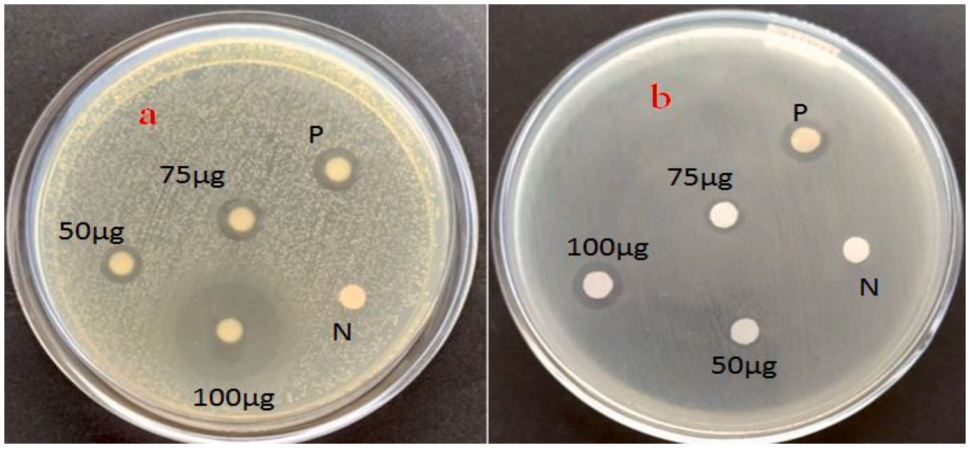

Fig. 6. Bacterial cultures showing the inhibition zones ZnO NPs. (a) *S. aureus* and (b) K. Pneumonia and P is positive and N is negative control respectively.

Table 1
Zone of Inhibition against selected bacteria (mm).

Type of pathogenic	Positive(Amoxillin-1 mg)	Zone inhibition 50 µg/ml	in mm 75 µg/ml	100 µg/ml
S. aureus (G+)	11	10	12	20.4
K. Pneumonia (G-)	9	6	8	11

of amine or amide groups. The peaks observed at 1228 cm^{-1} were associated with C—N stretching vibrations of aliphatic amines and 1037 cm^{-1} were assigned to the C—O vibration modes of the phenols and alcohols The absorption peaks in the region 1375 and 1037 cm^{-1} indicates the presence of C=C and C–O [44]. Furthermore, the peaks observe in the region between 600 and 400 cm^{-1} have been allocated to the metal–oxygen. So the high intensity band at 444 cm^{-1} is the result of the presence of the oxygen and zinc (Zn-O). As evidenced by the above results, Zinc oxide and plant secondary metabolites work well together. Results like these points to the possibility that biological substances like phenolic compounds and flavanoids can be used to act as a reducing and stabilizing agent during the formation of ZnO NPs.

3.3. XRD of ZnO NPs

The ZnO nanoparticles' phase and crystallinity are verified by capturing their X-ray diffraction pattern. Fig. 3 displays the XRD patterns for the ZnO NPs that were obtained. For the hexagonal wurtzite ZnO phase (JCPDS-file: 36–1451 [45], the diffraction peaks at 31.6°, 34.3°, 36.1°, 47.4°, 56.4°, 62.7°, 66.2°, 67.8°, and 69° could be attributed to lattice planes (h, l, k) of (100), (002), (101), (110), (103), (200), (112), and (201). In addition, the absence of an impurity peak in the diffraction pattern is indicative of full conversion of the Zn precursor into ZnO NPs. The phenols and flavonoids included in *P. alba* leaf extract function as a reducing agent and protect the zinc acetate molecule's outermost surface. Then, they prompted ZnO NPs to develop. Narrow and prominent diffraction peaks suggest that the product's particles have a well-defined crystalline structure. The produced ZnO NPs are highly crystalline, as evidenced by the strong peak intensity. The Scherrer formulas were used to make an approximation of the crystallite size (D).

$$D = \frac{K\lambda}{\beta \cos\theta} \quad (1)$$

Where k is the Scherrer's constant ($k = 0.94$), λ is the wavelength of the X-ray radiation, Θ is the Bragg's angle of the peak and β is FWHM (in radium). This XRD analysis proves *P. Alba* seeds are effective reducing agents for synthesized ZnO NPs. Particles were determined to have diameters in the 48 nm range after being calculated using the Scherrer formula.

3.4. XPS of ZnO NPs

The chemical composition of the produced samples was studied using X-ray photoelectron spectroscopy (XPS). The XPS spectra of the ZnO NPs are shown in Fig. 4. The survey spectrum of the matching ZnO NPs (see Fig. 4a) revealed just the Zn and O elements, demonstrating that the ZnO NPs are pure and devoid of metallic impurities.

Zn 2p and O 1 s spectra of pure ZnO are displayed in Fig. 4b and c, respectively. The existence of $Zn^{2+}$is confirmed by the occurrence of two peaks at 1021 and 1044 eV in the Zn 2p spectra, which are assigned to Zn 2p3/2 and Zn 2p1/2, respectively. According to the literature, the 23 eV gap between the two peaks is the correct value for the spin splitting energy separation. These agree very well with a typical binding energy of Zn^{2+}in ZnO [46]. The O 1 s are depicted in Fig. 5c. At 530 and 531.5 eV, two peaks were seen. The surface of the sample displays two distinct oxygen peaks. ZnO accounts for the 530 eV peak, whereas the 531.5 eV peaks are attributed to chemisorbed oxygen brought about by the presence of hydroxyl groups on the surface.

3.5. SEM of NPs

SEM images are used to make predictions about the shape of ZnO NPs. SEM images of ZnO NPs under different magnifications are displayed in Fig. 5a. Most of the ZnO NPs have an aggregated, aloe vera leaf form. Furthermore, Fig. 5b. shows Energy dispersive spectroscopy (EDS) of ZnO NPs which confirms the presence of Zinc and Oxygen.

Table 2
Comparison of antibacterial activity with other material.

Materials	Pathogens	Zone of inhibition in mm	Reference
ZnO using *Strychnos nux-vomica* L.	*S. aureus*	16	[2]
ZnO using *Phoenix roebelenii*	*S. aureus*	15	[5]
ZnO using *Chironji*	*S. aureus*	7	[17]
ZnO using *Canthium dicoccum* (L.)	*S. aureus*	15	[50]
ZnO using *Periconium* sp.	*S. aureus*	16	[51]
ZnO using *P.alba*	*S. aureus*	20.4	Present study

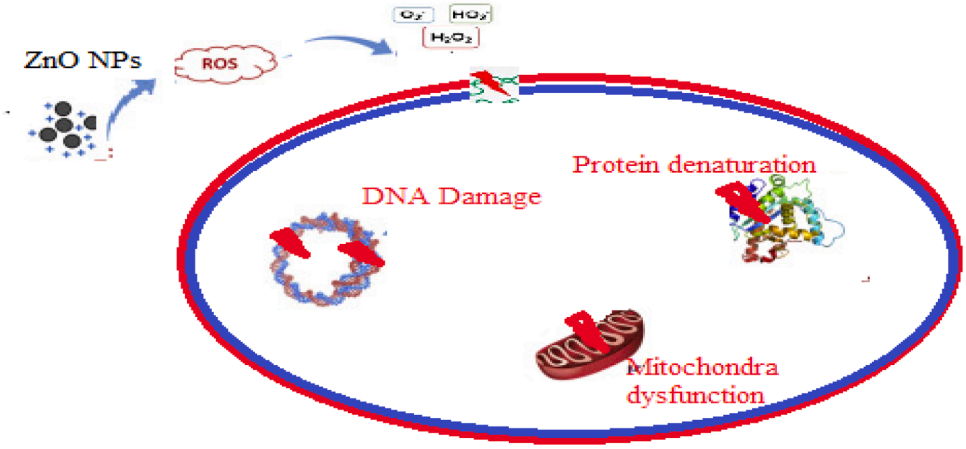

Scheme 1. Schematic representation of antibacterial mechanism.

3.6. Antibacterial activity

Different concentrations of the sample were tested against two pathogens, gram-positive (*S. aureus*) and gram-negative (*K. Pneumonia*), using the disc diffusion procedure.to determine the antibacterial activities of the green produced ZnO NPs. ZnO NP-induced inhibitory zones for gram-positive and gram-negative bacteria are shown in Fig. 6. Sizes of inhibitory zones, in millimetres, are shown in a Table 1. Drug Amoxillin was also used under for comparison of ZnO NPs. Distilled water was used as a negative control. ZnO NPs display significant antibacterial action, as seen by the 20.4 mm maximum inhibition zones reported for *S. aureus* and 11 mm the gram-negative bacterium *K. pneumophila*. The antimicrobial efficacy of ZnO NPs was concentration dependant. If more concentrations of NPs are present, the inhibitory zone will be more effective. The results reveal that the diameter of the inhibitory zone increases with increasing nanoparticle concentration for all tested strains and increasing ZnO concentration results in the decrease in the microbial cell growth [47]. It was also observed that the biosynthesized sample showed better antibacterial performance against grampositive bacteria when compared to gram-negative bacteria. Because Gram-positive bacterial cell wall is thicker and consists of peptidoglycan layers. The cell walls of gram-negative bacteria are physically and chemically more complicated than those of gram-positive bacteria.

However, it is not yet known how these compounds exert their antibacterial effects. Here, the presence of ZnO NPs leads to damages to the cell wall of *S. aureus* (Scheme 1). This effect can be explained by the strong direct interactions with bacterial membrane surface and antibacterial agent like ZnO NPs. In order for the ZnO NPs to penetrate the bacteria's cells, the bacteria's membrane keeps small pores. ZnO NPs cause cell harm by encouraging microorganisms to emit reactive oxygen species once they have broken through a membrane. Moreover, the samples generated form $e^{-}h^{+}$ pairs when irradiated with light, and these pairs are reactive oxygen species that can damage DNA and proteins, ultimately leading to the death of the bacterial cells. Due to ZnO NPs narrowing bandgap, its ability to generate reactive oxygen species (ROS) is diminished. These findings demonstrate that ZnO NPs are hazardous to the tested bacterial strains [48]. This means they have great potential as an antibacterial agent in commercial and medical settings.

The antibacterial activity of other catalysts are given in Table 2. Comparison of the results indicates that our catalytic system exhibits better antibacterial activity

4. Conclusion

In this work, researcher present a greener technique for synthesizing ZnO NPs by extracting its bioactive components from *P. alba* leaf which is simple, environmentally friendly, nontoxic, and biological method. Polyphenols are abundant in *P. alba* leaf extract, which serves as a reducing and capping agent in ZnO NPs production. UV–Vis, FT-IR, XRD, FE-SEM with EDS, and XPS were used to examine the morphological and structural characteristics of the produced ZnO NPs. Results from the ultraviolet to visible range show that the peak absorbence occurs at 375 nm, corresponding to an energy gap of 2.96 eV. XRD analysis indicated a mean particle size of 48 nm. Electron microscopy pictures revealed the development of polydispersed and aloe-vera leaf like NPs. Antimicrobial activity was shown in the green produced ZnO NPs against Gram-positive (*S. aureus*) and Gram-negative (*K. Pneumonia*) bacteria.

Declaration of Competing Interest

The authors declare that they have no known competing financial interests or personal relationships that could have appeared to influence the work reported in this paper.

Data availability

The data that has been used is confidential.

References

[1] F. Sanchez, K. Sobolev, Nanotechnology in concrete – a review, Constr. Build. Mater. 24 (2010) 2060–2071.
[2] K. Steffy, G. Shanthi, A.S. Maroky, S. Selvakumar, Synthesis and characterization of ZnO phytonanocomposite using Strychnos nux-vomica L. (Loganiaceae) and antimicrobial activity against multidrug-resistant bacterial strains from diabetic foot ulcer, J. Adv. Res. 9 (2018) 69–77.
[3] M. Rizwan, S. Ali, M.F. Qayyum, Y.S. Ok, M. Adrees, M. Ibrahim, M.Z. Rehman, M. Farid, F. Abbas, Effect of metal and metal oxide nanoparticles on growth and physiology of globally important food crops: a critical review, J. Hazard. Mater. 322 (2016) 2–16.
[4] G. Sangeetha, S. Rajeshwari, R. Venckatesh, Green synthesis of zinc oxide nanoparticles by aloe barbadensis miller leaf extract: Structure and optical properties, Mater. Res. Bull. 46 (2011) 2560–2566.
[5] T.S. Aldeen, H.E.A. Mohamed, M. Maaza, ZnO nanoparticles prepared via a green synthesis approach: physical properties, photocatalytic and antibacterial activity, J. Phys. Chem. Solids 160 (2022) 110313.
[6] A. Dey, Semiconductor metal oxide gas sensors: a review, Mater. Sci. Eng. B 229 (2018) 206–217.
[7] A.B. Djurišić, Y.H. Leung, A.M.C. Ng, Strategies for improving the efficiency of semiconductor metal oxide photocatalysis, Mater. Horiz. 1 (2014) 400–410.
[8] N. Bala, M. Sarkar, M. Maiti, P. Nandy, R. Basud, S. Das, Phenolic compound-mediated single-step fabrication of copper oxide nanoparticles for elucidating their influence on anti-bacterial and catalytic activity, New J. Chem. 41 (2017) 4458–4467.
[9] S.P. Meshram, P.V. Adhyapak, U.P. Mulik, D.P. Amalnerkar, Facile synthesis of CuO nanomorphs and their morphology dependent sunlight driven photocatalytic properties, Chem. Eng. J. 204–206 (2012) 158–168.
[10] D. Suresh, R.M. Shobharani, P.C. Nethravathi, M.A.P. Kumar, H. Nagabhushana, Artocarpus gomezianus aided green synthesis of ZnO nanoparticles: luminescence, photocatalytic and antioxidant properties 141 (2015) 128–134.
[11] P. Rajiv, S. Rajeshwari, R. Venckatesh, Bio-Fabrication of zinc oxide nanoparticles using leaf extract of Parthenium hysterophorus L. and its size-dependent antifungal activity against plant fungal pathogens, Spectrochim. Acta A Mol. Biomol. Spectrosc. 112 (2013) 384–387.
[12] S. Iravani, Green synthesis of metal nanoparticles using plants, Green Chem. 13 (2011) 2638–2650.
[13] N. Salaha, W.M. AL-Shawafi, A. Alshahriea, N. Baghdadia, Y.M. Solimanb, A. Memica, Size controlled, antimicrobial ZnO nanostructures produced by the microwave assisted route, Mater. Sci. Eng. C 99 (2019) 1164–1173.
[14] R. Gill, S. Ghosh, A. Sharma, D. Kumar, V.H. Nguyen, D.V.N. Vo, T.D. Pham, P. Kumar, Vertically aligned ZnO nanorods for photoelectrochemical water splitting application, Mater. Lett. 277 (2020) 128295.
[15] M. Chennimalai, V. Vijayalakshmi, T.S. Senthil, N. Sivakumar, One-step green synthesis of ZnO nanoparticles using Opuntia humifusa fruit extract and their antibacterial activities, Mater. Today 47 (2021) 1842–1846.
[16] A. Krol, V. Railean-Plugaru, P. Pomastowski, B. Buszewski, Phytochemical investigation of Medicago sativa L. extract and its potential as a safe source for the synthesis of ZnO nanoparticles: the proposed mechanism of formation and antimicrobial activity, Phytochem. Lett. 31 (2019) 170–180.
[17] S. Ju, K. Lee, M.H. Yoon, A. Facchetti, T.J. Marks, D.B. Janes, High performance field-effect transistors fabricated with laterally grown ZnO nanorods in solution, Nanotechnology 22 (2011) 185–310.
[18] D. Suresh, P.C. Nethravathi, Udayabhanu, M.A.P. Kumar, H.R. Naika, H. Nagabhushana, S.C. Sharma, Chironji mediated facile green synthesis of ZnO nanoparticles and their photoluminescence, photodegradative, antimicrobial and antioxidant activities, Mater. Sci. Semicond. Proc. 40 (2015) 759–765.
[19] C.B. Ong, L.Y. Ng, A.W. Mohammad, A review of ZnO nanoparticles as solar photocatalysts: synthesis, mechanisms and applications, Renew. Sustain. Energy Rev. 81 (2018) 536–551.
[20] S.E. Cross, B. Innes, M.S. Roberts, T. Tsuzuki, Human skin penetration of sunscreen nanoparticles: in-vitro assessment of a novel micronized zinc oxide formulation, Skin Pharmacol. Physiol. 20 (2007) 148–154.
[21] C. Dagdeviren, S.W. Hwang, Y. Su, S. Kim, Transient, biocompatible electronics and energy harvesters based on ZnO, Small 9 (2013) 3398–3404.
[22] H. Singh, A. Kumar, A. Thakur, P. Kumar, V.H. Nguyen, D.V.N. Vo, A. Sharma, D. Kumar, One-pot synthesis of magnetite-ZnO nanocomposite and its photocatalytic activity, Top. Catal. 63 (2020) 1097–1108.
[23] D. Skoda, P. Urbanek, J. Sevcik, L. Munster, J. Antos, I. Kuritka, Microwave-assisted synthesis of colloidal ZnO nanocrystals and their utilization in improving polymer light emitting diodes efficiency, Mater. Sci. Eng. B 232–235 (2018) 22–32.
[24] W. Gao, Z. Li, ZnO thin films produced by magnetron sputtering, Ceram. Int. 30 (2004) 1155–1159.
[25] J. Yu, X. Yu, Hydrothermal synthesis and photocatalytic activity of zinc oxide hollow spheres, Environ. Sci. Technol. 42 (2008) 4902–4907.
[26] S.J. Ikhmayies, Synthesis of ZnO microrods by the spray pyrolysis technique, J. Electron. Mater. 45 (2016) 3964–3969.

[27] S. Bhat, S.V. Shrisha, K.G. Naik, Synthesis of ZnO nanostructure by solvothermal method, Arch. Phy. Res. 4 (2013) 61–66.
[28] R. Perveena, S. Shujaata, Z. Qureshib, S. Nawazc, M.I. Khand, M. Iqbal, Mater. Sci. Energy Technol. 3 (2020) 335–343.
[29] M. Pattanayak, P.L. Nayak, Ecofriendly green synthesis of iron nanoparticles from various plants and spices extract, Int. J. Plant Anim. Environ. Sci. 3 (2013) 78–86.
[30] S.A. Devi, M. Harshinya, S. Udaykumar, P. Gopinath, M. Matheswaran, Strategy of metal iron doping and green-mediated ZnO nanoparticles: dissolubility, antibacterial and cytotoxic traits, Toxicol. Res. 6 (2017) 854–865.
[31] K.B. Narayanan, N. Sakthivel, Green synthesis of biogenic metal nanoparticles by terrestrial and aquatic phototrophic and heterotrophic eukaryotes and biocompatible agents, Adv. Colloid Interface Sci. 169 (2011) 59–79.
[32] M. Sundrarajan, S. Ambika, K. Bharathi, Plant-extract mediated synthesis of ZnO nanoparticles using Pongamia pinnata and their activity against pathogenic bacteria, Adv. Powder Technol. 26 (2015) 1294–1299.
[33] G. Benelli, Plant-borne compounds and nanoparticles: challenges for medicine, parasitology and entomology, Environ. Sci. Pollut. Res. 25 (2018) 10149–10150.
[34] J. Santhoshkumar, S.V. Kumar, S. Rajeshkumar, Synthesis of zinc oxide nanoparticles using plant leaf extract against urinary tract infection pathogen, Resour. Technol. 3 (2017) 459–465.
[35] I. Bibi, N. Nazar, M. Iqbal, S. Kamal, H. Nawaz, S. Nouren, Green and eco-friendly synthesis of cobalt-oxide nanoparticle: characterization and photo-catalytic activity, Adv. Powder Technol. 28 (2017) 2035–2043.
[36] S. Rashmi, V. Preeti, Biomimetic synthesis and characterisation of protein capped silver nanoparticles, Bioresour. Technol. 100 (2009) 501–504.
[37] K. Elumala, S. Velmurugan, Green synthesis, characterization and antimicrobial activities of zinc oxide nanoparticles from the leaf extract of Azadirachta indica (L.), Appl. Surf. Sci. 345 (2015) 329–336.
[38] N. Bala, S. Saha, M. Chakraborty, M. Maiti, S. Das, R. Basu, P. Nandy, Green synthesis of zinc oxide nanoparticles using Hibiscus subdariffa leaf extract: effect of temperature on synthesis, anti-bacterial activity and anti-diabetic activity, RSC Adv. 5 (2015) 4993–5003.
[39] M. Arumugam, D.B. Manikandan, E. Dhandapani, A. Sridhar, K. Balakrishnan, M. Markandan, T. Ramasamy, Green synthesis of zinc oxide nanoparticles (ZnO NPs) using Syzygium cumini: potential multifaceted applications on antioxidants, cytotoxic and as nanonutrient for the growth of Sesamum indicum, Environ. Technol. Innov. 23 (2021) 101653.
[40] S. Yadurkar, C. Mourya, P. Maheswar, Biosynthesis of zinc oxide nanoparticles using ixora coccinea leaf extract—a green approach, J. Synth. Theory Appl. 5 (2016) 1–14.
[41] D. Suresh, P.C. Nethravathi, P.C. Udayabhanu, H. Rajanaika, H. Nagabhushana, S. C. Sharma, Green synthesis of multifunctional zinc oxide (ZnO) nanoparticles using Cassia fistula plant extract and their photodegradative, antioxidant and antibacterial activities, Mater. Sci. Semicond. Proc. 31 (2015) 77–86.
[42] N. Matinise, X.G. Fuku, K. Kaviyarasu, N. Mayedma, M. Maaza, ZnO nanoparticles via Moringa oleifera green synthesis: physical properties & mechanism of formation, Appl. Surf. Sci. 406 (2017) 339–347.
[43] G. Sharmila, C. Muthukumaran, E. Sangeetha, H. Saraswathi, S. Soundarya, N. M. Kumar, Nanostructure, green fabrication, characterization of *Pisonia Alba* leaf extract derived MgO nanoparticles and its biological applications, Nano Objects 20 (2019) 100380.
[44] S.S. Sana, D.V. Kumbhakar, A. Pasha, S.C. Pawar, A.N. Grace, R.P. Singh, V. H. Nguyen, Q.V. Le, W. Peng, Crotalaria verrucosa leaf extract mediated synthesis of zinc oxide nanoparticles: assessment of antimicrobial and anticancer activity, Molecules 25 (2020) 4896.
[45] S.S. Mydeen, R.R. Kumar, M. Kottaisamy, V.S. Vasantha, Biosynthesis of ZnO nanoparticles through extract from Prosopis juliflora plant leaf: antibacterial activities and a new approach by rust-induced photocatalysis, J. Saudi Chem. Soc. 24 (2020) 393–406.
[46] M. Ramesh, M. Anbuvannan, G. Viruthagiri, Green synthesis of ZnO nanoparticles using Solanum nigrum leaf extract and their antibacterial activity, Spectrochim. Acta Part A Mol. Biomol. Spectrosc. 136 (2015) 864–870.
[47] T.S. Aldeen, H.E.A. Mohamed, M. Maaza, ZnO nanoparticles prepared via a green synthesis approach: physical properties, photocatalytic and antibacterial activity, J. Phys. Chem. Solids 160 (2022) 110313.
[48] M.S. Jadhav, S. Kulkarni, P. Raikar, D.A. Barretto, S.K. Vootla, U.S. Raikar, Green biosynthesis of CuO & Ag–CuO nanoparticles from Malus domestica leaf extract and evaluation of antibacterial, antioxidant and DNA cleavage activities, New J. Chem. 42 (2018) 204–213.
[49] S. Kannaiyan, D. Easwaramoorthi, K. Kannan, A. Gopal, R. Lakshmipathy, K. M. Katubi, N.S. Almuaikel, I.L.R. Rico, *Pisonia Alba* assisted synthesis of nanosilver for wound healing activity, Bioinorg. Chem. Appl. 2022 (2022) 1775198.
[50] C. Mahendra, M.N. Chandra, M. Murali, M.R. Abhilash, S.S. Brijesh, S. Satish, M. S. Sudharsana, Phyto-fabricated ZnO nanoparticles from Canthium dicoccum (L.) for antimicrobial, anti-tuberculosis and antioxidant activity, Process Biochem 89 (2020) 220–226.
[51] V. Ganesan, M. Hariram, S. Vivekanandhan, S. Muthuramkumar, Periconium sp. (endophytic fungi) extract mediated sol-gel synthesis of ZnO nanoparticles for antimicrobial and antioxidant applications, Mater. Sci. Semicond. Proc. 105 (2020) 104739.